Energetics Analysis of Forms I−IV Syndiotactic Polypropylene Crystal Structures

Kim Palmo and Samuel Krimm*

Biophysics Research Division and Department of Physics, University of Michigan, Ann Arbor, Michigan 48109

Received July 16, 2001; Revised Manuscript Received October 28, 2001

ABSTRACT: A vibrationally accurate potential energy function, our spectroscopically determined force field (SDFF), is used to calculate the relative zero-point-corrected energies of various forms I−IV syndiotactic polypropylene (sPP) crystal structures, both in their unconstrained and room-temperature unit cells. The results confirm the instability of the pure *Ibca* structure and support suggestions that form I sPP may be a statistical mixture of structures. Form IV is shown to have an energy close to form I structures, making its participation in kink bands possible. The relatively high energy of the form III unit cell makes it understandable that this structure is found only under external tension.

Introduction

Syndiotactic polypropylene (sPP) has been known to exhibit an extensive polymorphism in its crystal chain conformation and unit cell packing arrangements. These variations have been elucidated primarily through experimental probes such as X-ray diffraction, electron diffraction and microscopy, and NMR spectroscopy, which have yielded compelling conclusions about the above structural features. Evidence for certain kinds of structural disorder has also been inferred from such data, although the specific nature of the disorder is probably less uniquely defined. Energetics calculations can be helpful in evaluating structural states, but so far those that have been done have depended on simplified potential energy functions and constraining boundary conditions. A more dependable analysis is desirable, and we have reexamined this issue using a spectroscopically accurate energy function that we have developed.

Structural studies have identified four presently recognized crystalline forms of sPP. Form I is the stable form obtained from melt, solution, and single-crystal crystallizations, and the chain structure was found to be based on a $(t_2g_2)_2$ conformation (corresponding to an s(2/1)2 helix).[1,2] However, the chain packing arrangement in the unit cell was not initially clear. The first detailed crystal structure analysis[3] proposed a *C*-centered orthorhombic cell with two isochiral chains (space group $C222_1$, now known as form II). Subsequent diffraction and microscopy studies[4−6] have shown that the unit cell is in fact doubled along the *b*-axis and consists of alternating right-handed (R) and left-handed (L) helices along this direction. This unit cell (space group *Ibca*) is orthorhombic, contains four chiral chains, and has unit cell parameters $a = 14.50$ Å, $b = 11.20$ Å, and c(chain axis) $= 7.40$ Å. Despite this advance in understanding, it was clear that the diffraction patterns could not be explained on the basis of the *Ibca* unit cell alone, and various types of packing disorder have been invoked to explain the discrepancies,[5,7−10] including the proposal of a monoclinic unit cell with chains rotated slightly about their axes.[9] Solid-state NMR studies[11,12] also provide evidence of departures from strict *Ibca* symmetry, although there may be a problem in distinguishing between a given chain conformation in different packing environments.[12,13] Possible specific structural variations were indicated by energetics calculations of *c*-axis shifts[14] as well as a full mapping of *b*-axis plus *c*-axis shifts[15] of *bc* sheets in the unit cell. These calculations[15] indicated that three structures ($\Delta b = 0.5b$, $\Delta c = 0$; $\Delta b = 0.196b$, $\Delta c = 0.5c$; $\Delta b = 0$, $\Delta c = 0.222c$) had slightly lower energies than the *Ibca* structure ($\Delta b = 0$, $\Delta c = 0$). However, neither of these alone, nor a proposed monoclinic variant with molecules rotated slightly about their axes,[9] provided an unambiguous explanation of small anomalies in the diffraction pattern.[16] It seems that some statistical mixing of structures[10,14,15] may be necessary to account for all of the features.

Form II, as noted above, is a *C*-centered orthorhombic unit cell of two isochiral $(t_2g_2)_2$ chains. It has the same *a*- and *c*-axis dimensions as the *Ibca* unit cell but half the *b*-axis dimension, viz., 5.60 Å. This form can be obtained by quench precipitation from solution[12,17] but is more generally produced in stretched samples,[3] particularly on release of the tension.[18] In fact, form II seems to develop from a crystal−crystal transformation in which a planar zigzag chain conformation (form III, see below) relaxes into form II.[19]

The presence of form III, based on a $(t_2)_2$ chain conformation, was first noted in samples that were cold-stretched after quenching from the melt.[20,21] Its crystal structure was subsequently determined[22] and consists of an orthorhombic unit cell with dimensions $a = 5.22$ Å, $b = 11.17$ Å, c(chain axis) $= 5.06$ Å, two chains per unit cell, and space group $P2_1cn$. It has been claimed that this form is obtained spontaneously by only quenching at 0 °C without stretching,[23−26] but others believe that a disorded lateral packing of all-trans chains, rather than the known crystalline form III,[22] is a better description of this state.[27]

Form IV was obtained by exposing samples prepared in the crystalline form III state to vapors of benzene, toluene, or *p*-xylene below 50° for several days.[28] Its crystal structure determination[28] established the chain conformation as based on $(t_6g_2t_2g_2)$, subsequently found to be consistent with NMR spectra,[29] and of three possible triclinic cells the preferred one had $a = 5.72$ Å, $b = 7.64$ Å, c(chain axis) $= 11.60$ Å, $\alpha = 73.1°$, $\beta = 88.8°$, $\gamma = 112.0°$ (the two others were $a = 5.94$ Å, $b =$

10.1021/ma011230g CCC: $22.00
Published on Web 12/13/2001

7.93 Å, $c = 11.60$ Å, $\alpha = 67.1°$, $\beta = 104.3°$, $\gamma = 116.8°$ and $a = 5.97$ Å, $b = 7.49$ Å, $c = 11.60$ Å, $\alpha = 102.5°$, $\beta = 106.5°$, $\gamma = 108.2°$). A recent reexamination of the crystal structure, incorporating packing energy as well as structure factor calculations,[30] indicates that a *C*-centered monoclinic cell, $a = 14.17$ Å, $b = 5.72$ Å, $c = 11.60$ Å, $\beta = 108.8°$, may be a better description of the packing arrangement.

The value of energetics calculations in gaining additional insights into sPP structure was recognized in the earliest investigations,[2,31] which indicated that periodic helical $(t_2g_2)_2$ and planar zigzag $(t_2)_2$ chain conformations had about the same energy. Subsequent calculations on such single chains,[32] based on explicit atoms, fixed bonds but variable bond angles and torsion angles, and later (although still simplified) energy functions,[33] showed that the planar zigzag is of slightly higher energy (0.65 kcal/mol/monomer unit) than the helical conformation. These calculations were extended to include packing energies of the chains in the crystal unit cells,[34−36] using the same energy functions.[33] A partial calculation of a distorted *Ibca* structure[14] was based on modifications of two empirical force fields, but the full mapping of the Δb and Δc shifts[15] was done with a spectroscopically determined force field (SDFF),[37] viz., a force field that in addition to structures and energies reproduces scaled ab initio vibrational frequencies to spectroscopic accuracy. (The two important additional components in the energy function that accomplish this, which are absent in the previously used function,[33] are bonded cross-terms and electrostatic interactions.)

The use of an SDFF is especially important in the case of the analysis of crystalline sPP structures. Because of the extensive polymorphism in this system, the energies per monomer unit (m.u.) are likely to be close in the various chain and crystal structures. It is therefore desirable to compare zero-point-corrected energies rather than just potential energies at the minima. Having an energy function that is designed for a self-consistent description of frequencies as well as structures and energies is therefore an advantage in achieving this goal.

In the following we describe the nature of our calculations and then discuss the results for the various single-chain conformations and then for the different crystal forms.

Calculations

The potential energy function for these calculations was our SDFF for the branched hydrocarbon chain.[38] (These parameters differ slightly from those used in the earlier sPP analysis[15] as a result of basing the potential on a redundant rather than a nonredundant set of internal coordinates.) This potential reproduces 21 ab initio hydrocarbon structures within rms deviations of <0.003 Å in bond lengths, $<0.5°$ in bond angles, and $<2.5°$ in torsion angles; 17 relative energies of conformers are reproduced with an average deviation of 0.2 kcal/mol; and the rms deviation for 791 non-CH stretching frequencies is 6.2 cm^{-1}, with 90% of the frequencies being within ± 10 cm^{-1} of the (scaled) ab initio values. The sPP calculations are for structures that are effectively infinite in extent along the chain axes (for single chains) as well as in the lateral directions (for the crystals), with nonbonded interactions being summed over a number of repeat units from a central one such that a minimum nonbonded cutoff distance is ∼30 Å. Increasing this distance has no significant effect on the results.

For calculations on single chains, a starting conformation close to the studied structure was chosen, but other than the requirement of chain axis periodicity no structural constraints were imposed on the system. (Thus, for the $(t_2g_2)_2$ structure the asymmetric unit was the four-monomer group.) The energy was minimized with respect to all coordinates (using our SPEAR program[39]), this value per monomer unit being designated as $E_0(0)$ (corresponding to a 0 K structure, i.e., one that excludes thermal vibrations), the frequencies at the minimum were calculated, and zero-point energies per m.u. were computed (as the sum of $^1/_2h\nu$ divided by the number of m.u.) to correct the $\Delta E_0(0)$ to give $\Delta E_z(0)$.

For the crystal lattices, two types of calculations were done: essentially unconstrained unit cells (corresponding to 0 K structures, which will generally give unit cell parameters smaller than those observed at room temperature) and ones in which the unit cell parameters were fixed at the experimental (room temperature, RT) values. (In the latter case, in contrast to an earlier calculation,[36] we do not increase the van der Waals radii of atoms to represent the anharmonic effects of increased thermal motion, since this destroys the internal self-consistency of the potential energy function. Although a proper treatment requires a statistical mechanical calculation,[40] we believe that the present approach at least gives a significant indication of how the structure adjusts to the altered intermolecular interactions in the enlarged unit cell.) In the case of the 0 K structures, imposed constraints were as follows. For the form I $(t_2g_2)_2$ structure, the *Ibca* symmetry element between adjacent (R and L) chains in a *bc* sheet was maintained as well as the symmetry element between adjacent sheets. In the four-monomer asymmetric unit, all Cartesian coordinates were allowed to vary, which, of course, allows for relative translations and rotations between adjacent chains in a *bc* sheet. The energy always minimizes at the chain arrangement in the *Ibca* sheet, and we thus agree with the observation[16] that any displacements "must involve entire *bc* sheets rather than individual molecules". Such a restriction of course does not apply to the form II unit cell. For the form III $(t_2)_2$ crystal structure, the only imposed constraint is the 2-fold axis relating the two chains in the observed unit cell.[22] For the form IV $(t_6g_2t_2g_2)$ triclinic crystal structure,[28] of course no constraints are imposed on the energy minimization, whereas for the monoclinic version[30] the *C*-centered structure with $\alpha = \gamma = 90°$, but no intrachain symmetry, was imposed. In the case of the RT form I structure, the symmetry within a *bc* sheet was maintained, the experimental *b* and *c* unit cell values were imposed, and *a*, α, β, and γ were allowed to vary under the constraint that the intersheet separation correspond to the experimental value of 7.25 Å. In all cases, frequencies were calculated for the entire unit cell and the zero-point energy per m.u. was used to correct $\Delta E_0(\mathrm{RT})$ to $\Delta E_z(\mathrm{RT})$.

Results and Discussion

1. Single-Chain Structures. Before considering the crystal structures, it is useful to determine the equilibrium conformations of the isolated chains. This helps to understand changes in chain conformation that result from interchain interactions in the crystal.

Table 1. Structures[a] and Energies[b] of Isolated Chains of Syndiotactic Polypropylene

parameter	structure		
	$(t_2g_2)_2$	$(t_2)_2$	$(t_6g_2t_2g_2)$
chain repeat	7.54	5.11	11.40
CC bonds[c]	1.542, 1.542, 1.545, 1.545, 1.542, 1.542, 1.545, 1.545	1.550, 1.550, 1.550, 1.550	1.543, 1.544, 1.545, 1.545, 1.544, 1.543, 1.544, 1.545, 1.543, 1.543, 1.545, 1.544
CCC angles[c]	111.7, 116.4, 111.7, 117.4, 111.7, 116.4, 111.7, 117.4	110.9, 113.5, 110.9, 113.5	112.0, 116.6, 108.4, 117.2, 108.4, 116.6, 112.0, 117.6, 111.8, 116.5, 111.8, 117.6
CC torsions[c]	−176.2, −176.2, 59.4, 59.4, −176.2, −176.2, 59.4, 59.4	162.4, 162.4, −162.4, −162.4	−176.8, −173.8, 177.1, 177.1, −173.8, −176.8, 57.5, 54.4, 179.0, 179.0, 54.4, 57.5
energies			
$E_0(0)$[cov][d]	0.75	1.23	0.72
$E_0(0)$[vdW][e]	1.68	2.31	1.76
$E_0(0)$[elec][f]	−11.86	−11.87	−11.81
$E_0(0)$	−9.43	−8.33	−9.33
$\Delta E_0(0)$	0	1.10	0.10
$\Delta E_z(0)$[g]	0	0.94	0.10

[a] Bond lengths in angstroms; bond angles and torsions in degrees. [b] Energies in kcal/mol/m.u. [c] Main chain: first bond (corresponding to central bond of the first torsion) starts at CH−CH_2, first angle starts at same CH_2−CH−CH_2, first torsion starts at CH−CH_2 bond. [d] Energy of distortion of bonds, angles, and torsions (including cross-terms), from intrinsic values.[38] [e] Intrachain van der Waals energy. [f] Intrachain electrostatic energy. [g] Total relative zero-point-corrected energy.

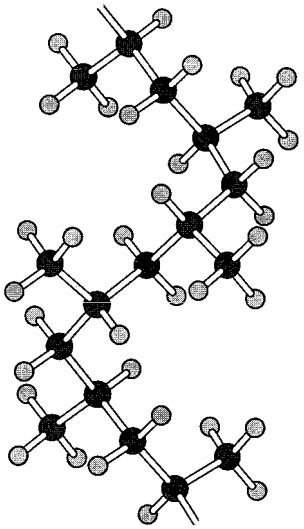

Figure 1. Minimized energy $(t_2g_2)_2$ single-chain structure.

(a) $(t_2g_2)_2$ Chain. The total potential energy, $E_0(0)$, and its covalent, van der Waals, and electrostatic components of the equilibrium right-handed $(t_2g_2)_2$ chain are given in Table 1. The structural parameters are also given in Table 1, and the chain conformation is illustrated in Figure 1. Several features of this SDFF-calculated 0 K structure are noteworthy. The conformation clearly exhibits the expected s(2/1)2 symmetry without this condition being imposed as a prior constraint.[32,35,36] The CC bonds obviously cannot be expected to have a constant length, as has been assumed.[9,32−36] (Although the bond length differences are very small, these can lead to larger differences in bond angles and bond torsions, which mainly determine the chain axis repeat.) All CCC main chain bond angles are not equal: although we find, as others,[35,36] that the CH_2−CH(CH_3)−CH_2 angle is smaller than the C−CH_2−C angles, our calculations show that the C−g-CH_2−g-C angle (117.4°) is larger than the C−t-CH_2-t−C angle (116.4°) whereas a recent calculation[36] gives the opposite result (114.7° vs 115.0°). The torsion angles (−176.2° and 59.4°) are significantly different from those recently proposed: 175.2° and 66.7° in one case,[35] 180.3° and 62.0° in another.[36] The chain axis repeat (7.54 Å) is significantly closer to the RT crystal value (7.40 Å) than a previously calculated unconstrained value (7.80 Å),[35] although a later calculation gives about the same value (7.52 Å).[36] (The comparison of our unconstrained structural parameters with those in ref 36 should be evaluated in the light of the constraints in the latter case, viz., methyl groups treated as "single units" and a "fixed chain configuration".)

We have emphasized that the SDFF energy function is designed to give spectroscopically acceptable vibrational frequencies as well as predicting accurate structures and energies. It is therefore of interest to examine the quality of this agreement for $(t_2g_2)_2$ sPP. Excellent infrared (IR)[41] and Raman (R)[42] spectra have been obtained for this material, and a careful normal-mode analysis based on an empirical spectroscopic force field has been done.[43] In the range ∼290−1340 cm^{-1}, where reasonable comparable assignments can be made, this analysis yields an rms error of 13.3 cm^{-1} while our SDFF gives frequencies that have an rms error of 8.4 cm^{-1} compared to the observed. (Although the observed spectra correspond to crystal rather than single-chain frequencies, our calculated frequencies for the crystal are within a few cm^{-1} of the single-chain values.) Some of this improvement may be due to the fact that a canonical $(t_2g_2)_2$ structure (i.e., t = 180°, g = 60°) was used in the earlier analysis,[43] whereas the actual conformation departs slightly from this (see Table 1). Bands characteristic of this conformation[1,3] are very well reproduced, the observed (and calculated) values being 810 (811), 868 (857), 977 (983), and 1005 (1005) cm^{-1}. In the lower frequency region, the spectroscopic analysis[43] seems to give very poor agreement whereas our SDFF does very well: calculated (observed IR, R) values (in the region where there is no interference from lattice modes) are 148 (147, −); 186 (166, 172); 197 (−, 200); 199 (206, −); 238, 245 (240, −); 251, 263, 267 (262, 260) cm^{-1}. Such overall good agreement ensures the reliability of our zero-point energy corrections.

(b) $(t_2)_2$ Chain. The energies and structural parameters of the $(t_2)_2$ chain are given in Table 1, and the conformation is illustrated in Figure 2. The potential energy per m.u. is 1.10 kcal/mol higher than that of the $(t_2g_2)_2$ chain, with the zero-point energy correction reducing this to 0.94 kcal/mol. No assumption is made about the chain symmetry (i.e., the asymmetric unit is the two-monomer group), yet the expected t*cm* symmetry is the result.[35] The chain geometry differs slightly from that previously calculated,[35] and there is no

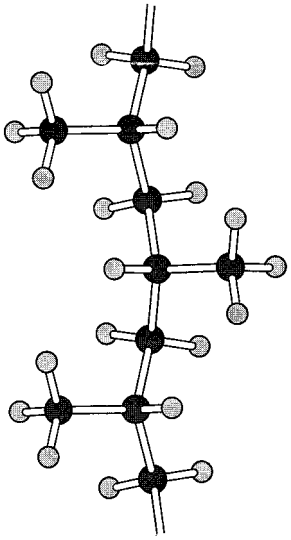

Figure 2. Minimized energy $(t_2)_2$ single-chain structure.

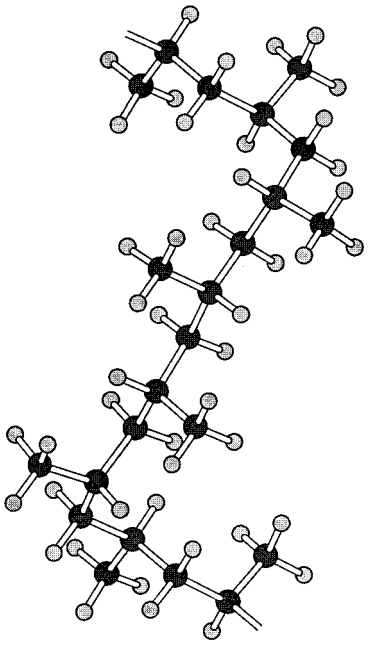

Figure 3. Minimized energy $(t_6g_2t_2g_2)$ single-chain structure.

evidence of the "tilted" CH_3 groups suggested by the crystal structure analysis.[22] The frequency agreement with observed IR bands[41] is better than that given by a spectroscopic normal-mode analysis[43] (rms error of 13.6 vs 20.1 cm^{-1}), perhaps because a strictly planar zigzag chain was assumed in the latter case.

(c) $(t_6g_2t_2g_2)$ Chain. The energies and structural parameters of the $(t_6g_2t_2g_2)$ chain are given in Table 1, and its conformation is illustrated in Figure 3. The potential energy per m.u. is 0.10 kcal/mol higher than that of the $(t_2g_2)_2$ chain, and the zero-point energy difference is the same. The bond lengths are in the range of those found from the initially proposed (RT) structure,[28] but the ranges for the bond angles and torsions differ slightly. The values of the trans torsion angles vary significantly along the chain. The structure does, however, exhibit the expected *t*2 symmetry,[30] i.e., 2-fold axes perpendicular to the chain axis through CH_2 carbons in the center of the t_6 and t_2 sequences, without this having been imposed on the optimization.

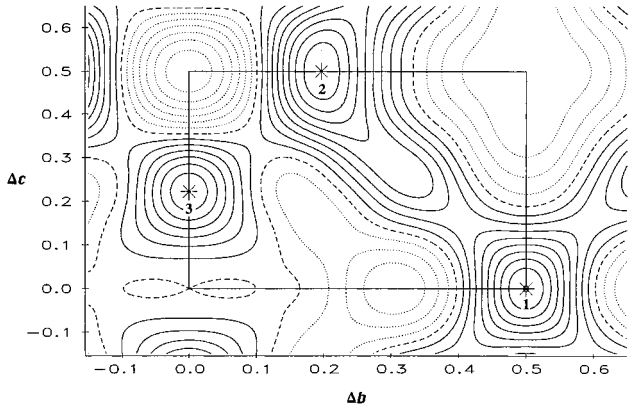

Figure 4. Energy surface for an orthorhombic cell as a function of fractional *b* and *c* unit cell displacements of *bc* sheets from the *Ibca* structure (at $\Delta b = \Delta c = 0$ and of zero energy). Contours are at 0.5 kcal/mol/unit cell; negative energies are shown by solid lines, zero energy by a broken line, and positive energies by dotted lines. From ref 15.

2. Crystal Structures. (a) Form I. We have already shown[15] that, in the context of an otherwise unconstrained orthorhombic cell of the *Ibca* type, there are three minima in the Δb, Δc arrangement of the *bc* sheets. This energy map is shown in Figure 4, with the minima now labeled in arabic numerals (to avoid confusion with the roman designations of the forms). The *Ibca* structure, i.e., $\Delta b = \Delta c = 0$, is, as has been noted,[14,15] at an energy maximum, and this is further confirmed by our finding that the unit cell has one imaginary frequency (12.3i cm^{-1}). Thus, this unit cell is unstable and, as evident from Figure 4, will tend to rearrange in the directions of minima 1, 2, and 3.

This rearrangement can take place in at least two ways:[14] the initial shift between the first and second *bc* sheets could be reversed between the second and third sheets, giving rise to an essentially orthorhombic cell (designed as an A cell), or the shift could be continued from sheet to sheet, which would lead to a reduced unit cell symmetry (designated as a B cell). We represent these situations in Figure 5 for shifts corresponding to each of the minima of Figure 4, and in Table 2 we give the results of energy optimizations for these structures.

The different unconstrained structures show some interesting variations. The A unit cells, as expected, are orthorhombic or nearly so, whereas the B unit cells are monoclinic. In all cases, the intersheet spacing is nearly the same, 6.92 ± 0.06 Å. The different intersheet arrangements, however, result in slightly different (even though internally regular) chain conformations. Only one of these (**1A**) has a chain torsion angle sequence $(t_1t_1g_1g_1t_1t_1g_1g_1)$ the same as that of the single chain (see Table 1), and it is not one of lowest potential energy (by 0.03 kcal/mol/m.u., or ∼0.5 kcal/mol per unit cell), although it is the lowest after the zero-point energy correction. Thus, a comparison of the energetics of different packing arrangements,[36] or of the resulting X-ray diffraction patterns,[16] cannot strictly be based on a common chain conformation. (Whether such differences can account for the appearance of reflections forbidden by the exact *Ibca* structure,[5] particularly if a mixing of sheet packings occurs,[15] remains to be determined.) The 4+ kcal/mol/m.u. difference between $E_0(0)$ for the crystal structures and that for the single chain highlights the significant impact of intermolecular interactions in stabilizing the structure despite the

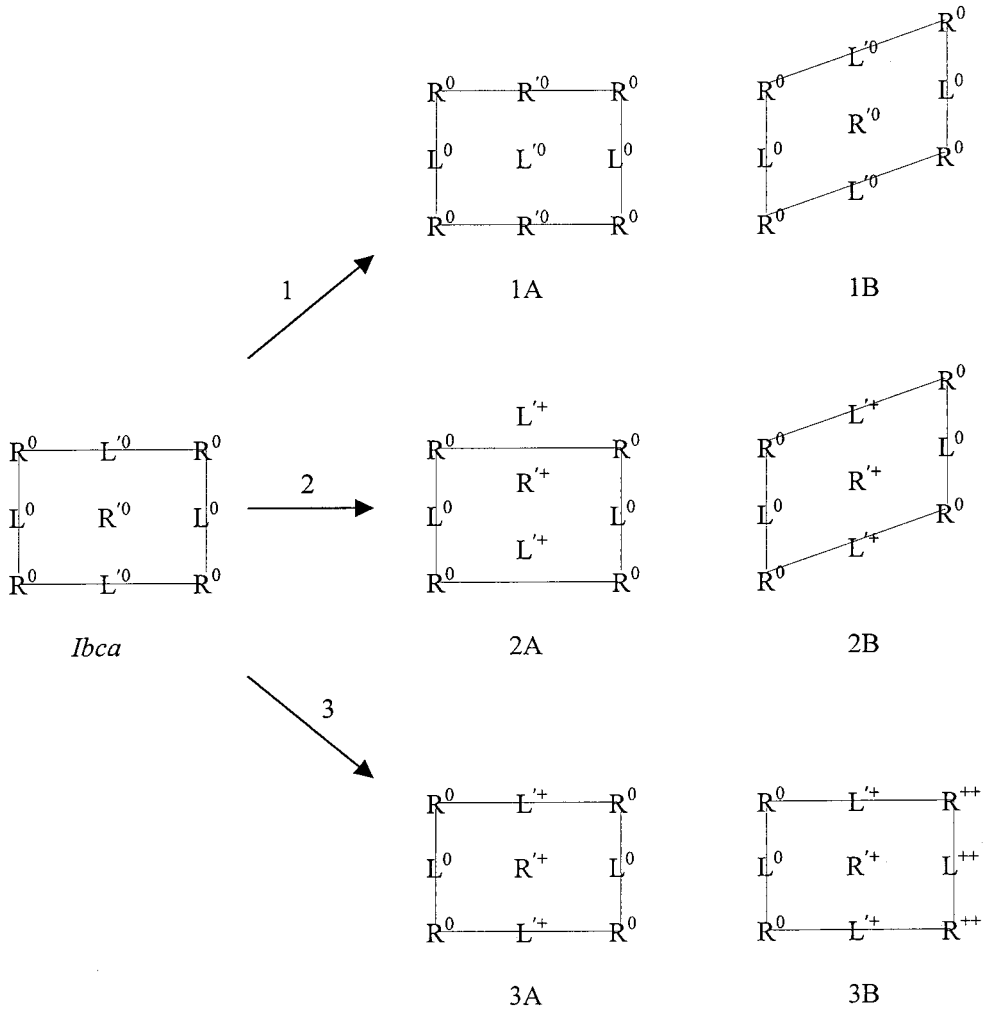

Figure 5. Form I crystal structures derived from energy minima 1, 2, and 3 of Figure 4. *Ibca* structure: R, right-handed chain; L, left-handed chain, ^{0}, initial *c*-axis relation of chains; $'$, symmetry-related *c*-axis shift of chains in second *bc* sheet compared to first (similar shift between second and third sheet results in equivalence of third and first sheets). A structures: *b* and *c* translations of alternate *bc* sheets are identical (i.e., translation between first and second sheets from *Ibca* structure is reversed between second and third). B structures: *b* and *c* translations of adjacent *bc* sheets are identical (i.e., translation from second to third sheet is the same as from first to second). $^+$: *c*-axis shift from *Ibca* structure corresponding to energy minimum (2 or 3).

slight increase in intramolecular chain energy in the crystal (−9.41 vs −9.43 kcal/mol/m.u.). The relative E_z-(0) indicate that structures **1A** and **2B** would be highly competitive (although at room temperature structure **2B** is unstable; see below), with structure **2A** being only 0.03 kcal/mol/m.u. behind. Structures **3A** and **3B** are 0.10 and 0.12 kcal/mol/m.u. higher in energy, and structure **1B**, which equilibrates from the unstable *Ibca* (which has an energy of 0.37 kcal/mol/m.u.) by forming a monoclinic cell, is 0.21 kcal/mol/m.u. higher in energy (or ∼3.4 kcal/mol/unit cell).

The RT structures form unit cells very similar in symmetry to the unconstrained, although only three (**1A**, **2A**, and **3A**) retain the same chain torsion angle sequence as in the unconstrained cells. Structure **2B** has two imaginary frequencies, 9.3i and 5.1i cm^{-1}, and is therefore unstable under these conditions. Structure **1A** is still the lowest in energy, with structure **2A** being 0.05 kcal/mol/m.u. higher in relative energy. Structure **1B** is now even more unfavorable, with a relative energy of 0.36 kcal/mol/m.u. (The *Ibca* structure still has an imaginary frequency, making it unstable, and its energy of 0.35 kcal/mol/m.u is 0.23 kcal/mol/m.u. higher than that of structure **1A**.)

It is of interest to compare these results with departures from an exact *Ibca* structure that are inferred from diffraction studies. We note first that our RT results, in indicating that structures **1A**, **2A**, and **3A** would dominate energetically, support the observation that the form I unit cell is found to be orthorhombic. We do not find any evidence, in either the unconstrained or the RT structures, that chains are rotated around their axes[9] or that there is a *c*-axis shift of consecutive chains in a *bc* sheet.[9] A *c*-axis shift of adjacent *bc* sheets[5,9] is, however, consistent with minima 2 and 3 (see Figure 4), with the proposed *b*-axis shift invoked to account for defects[5] particularly favored by minimum 2. The situation is, of course, more complex if in fact the true structure embodies a statistical mixing of structures such as **1A**, **2A**, and **3A**.[15] (In such a case, the 0.25b shift indicated by the diffraction data[5] may prevail over the 0.2b shift, i.e., minimum 2, indicated for the pure structure **2A** unit cell.)

(b) Form II. As noted above, the form II crystal structure is based on the $(t_2g_2)_2$ sPP chain, with the unit cell consisting of two isochiral chains in *C*-centered orthorhombic symmetry. The structural parameters and

Table 2. Structures[a] and Energies[b] of Form I Crystalline Syndiotactic Polypropylene

	structure[c]					
parameter	**1A**	**1B**	**2A**	**2B**	**3A**	**3B**
unconstrained structures						
a	13.85	14.11 [13.97]	13.76 [13.75]	14.41 [13.62]	13.90	14.38 [13.98]
b	10.62	10.62	10.58	10.63	10.58	10.57
c	7.65	7.62	7.63	7.66	7.59	7.59
α	90.0	90.0	90.0	90.0	90.0	90.0
β	90.0	90.0	92.4	90.0	90.0	76.5
γ	90.0	81.8	90.0	71.0	89.2	90.0
Δb[d]	0.50	0.09	0.21	0.22	0	0
Δc[d]	0	0	0.50	0.50	0.22	0.22
CC bonds[e]	1.541, 1.541	1.541, 1.541	1.541, 1.541	1.541, 1.541	1.542, 1.542	1.542, 1.542
	1.542, 1.542	1.543, 1.543	1.543, 1.543	1.543, 1.543	1.543, 1.543	1.544, 1.543
	1.541, 1.541	1.541, 1.541	1.541, 1.541	1.541, 1.541	1.542, 1.542	1.541, 1.541
	1.542, 1.542	1.543, 1.543	1.543, 1.543	1.543, 1.543	1.543, 1.543	1.543, 1.544
CCC angles[e]	111.7, 116.1	111.7, 116.1	112.0, 115.9	111.7, 116.1	111.9, 115.9	111.9, 116.0
	111.7, 117.6	111.8, 117.0	112.0, 117.2	111.6, 117.3	111.8, 117.1	111.9, 117.1
	111.7, 116.1	111.7, 116.1	111.3, 116.5	111.7, 116.1	111.9, 115.9	111.7, 115.9
	111.7, 117.6	111.8, 117.0	111.3, 117.2	111.6, 117.3	111.8, 117.1	111.7, 117.1
CC torsions[e]	−177.6, −177.6	−178.4, −177.1	−178.4, −178.4	−177.4, −179.0	−174.8, −179.0	−176.6, −176.6
	61.1, 61.1	61.7, 60.3	60.9, 61.3	61.0, 61.8	60.5, 60.2	59.9, 60.7
	−177.6, −177.6	−178.4, −177.1	−177.5, −177.5	−177.3, −179.0	−174.8, −179.0	−177.2, −177.2
	61.1, 61.1	61.7, 60.3	61.3, 60.9	61.0, 61.8	60.5, 60.2	60.7, 59.9
energies						
$E_0(0)$[cov][f]	0.65	0.65	0.65	0.65	0.65	0.64
$E_0(0)$[vdW][g]	1.82	1.83	1.83	1.83	1.84	1.83
$E_0(0)$[elec][h]	−11.88	−11.87	−11.86	−11.87	−11.87	−11.87
$E_0(0)$[lat][i]	−4.35	−4.18	−4.38	−4.40	−4.31	−4.27
$E_0(0)$	−13.76	−13.57	−13.76	−13.79	−13.69	−13.67
$\Delta E_0(0)$	0.03	0.22	0.03	0	0.10	0.12
$\Delta E_z(0)$[g]	0	0.21	0.03	0.00[k]	0.10	0.12
room-temp structures						
a	14.5	15.0 [14.5]	14.5	16.1 [14.5]	14.5	15.1 [14.5]
b	11.2	11.2	11.2	11.2	11.2	11.2
c	7.4	7.4	7.4	7.4	7.4	7.4
α	90.0	90.0	90.0	90.0	90.0	90.0
β	90.0	90.0	90.0	90.0	90.0	74.5
γ	90.0	75.2	90.0	64.4	90.0	90.0
Δb[d]	0.50	0.17	0.19	0.28	0	0
Δc[d]	0	0	0.50	0.50	0.21	0.26
CC bonds[e]	1.541, 1.541	1.541, 1.540	1.541, 1.541	1.541, 1.540	1.541, 1.541	1.541, 1.541
	1.544, 1.544	1.545, 1.545	1.545, 1.545	1.544, 1.544	1.545, 1.545	1.545, 1.545
	1.541, 1.541	1.541, 1.540	1.541, 1.541	1.541, 1.540	1.541, 1.541	1.541, 1.541
	1.544, 1.544	1.545, 1.545	1.545, 1.545	1.544, 1.544	1.545, 1.545	1.545, 1.545
CCC angles[e]	111.3, 116.7	111.0, 116.9	111.4, 116.6	111.1, 116.7	111.3, 116.7	111.2, 116.7
	111.3, 117.1	111.0, 116.5	111.4, 116.9	111.3, 116.9	111.3, 116.9	111.2, 116.8
	111.3, 116.7	111.0, 116.9	111.1, 116.9	111.1, 116.7	111.3, 116.7	111.2, 116.8
	111.3, 117.1	111.0, 116.5	111.1, 116.9	111.3, 116.9	111.3, 116.9	111.2, 116.8
CC torsions[e]	−175.7, −175.7	−177.0, −177.3	−176.1, −176.1	−175.6, −176.5	−174.8, −176.9	−176.2, −176.2
	58.0, 58.0	58.7, 58.7	58.0, 58.3	57.9, 58.5	58.0, 58.2	58.2, 58.4
	−175.7, −175.7	−177.0, −177.3	−175.8, −175.8	−175.6, −176.5	−174.8, −176.9	−176.3, −176.3
	58.0, 58.0	58.7, 58.7	58.3, 58.0	57.9, 58.5	58.0, 58.2	58.4, 58.2
energies						
E_0(RT)[cov][f]	0.72	0.67	0.70	0.69	0.71	0.68
E_0(RT)[vdW][g]	1.73	1.80	1.75	1.77	1.75	1.78
E_0(RT)[elec][h]	−11.86	−11.84	−11.85	−11.86	−11.86	−11.85
E_0(RT)[lat][i]	−4.03	−3.92	−4.01	−3.90	−3.99	−3.96
E_0(RT)	−13.44	−13.29	−13.41	−13.30	−13.39	−13.35
ΔE_0(RT)[l]	0.35	0.50	0.38	0.49	0.40	0.44
ΔE_z(RT)[m]	0.12	0.36	0.17	0.30[n]	0.19	0.25

[a] Bond and unit cell lengths in angstroms; bond and unit cell angles, and torsions, in degrees. [ ]: separation between adjacent sheets. [b] Energies in kcal/mol/m.u. [c] See Figure 5. [d] Fractional unit cell shifts of *bc* sheets from *Ibca* structure. [e] Main chain: first bond (corresponding to central bond of the first torsion) starts at $CH-CH_2$, first angle starts at same $CH_2-CH-CH_2$, first torsion starts at $CH-CH_2$ bond. [f] Energy of distortion of bonds, angles, and torsions (including cross-terms) of a single chain from intrinsic values.[38] [g] Intrachain van der Waals energy. [h] Intrachain electrostatic energy. [i] Interchain van der Waals plus electrostatic energy. [j] Total relative zero-point-corrected energy. [k] Actual value relative to **1A**: 0.002. [l] Energy relative to $E_0(0)$ of **2B**. [m] Energy relative to $E_z(0)$ of **1A**. [n] This structure has two imaginary frequencies, 9.3i and 5.1i cm^{-1}.

energies of the unconstrained and RT structures are given in Table 3.

The unconstrained chain conformation maintains the $t_1t_1g_1g_1t_1t_1g_1g_1$ torsion angle sequence of the single chain (as was also the case for form I, **1A**), but the values of the trans and gauche angles are significantly different. The total energy is higher (0.21 kcal/mol/m.u.) than that of form I, **2B**, but after the zero-point energy correction

Table 3. Structures[a] and Energies[b] of Form II Crystalline Syndiotactic Polypropylene

	structure	
parameter	unconstrained	room temp
a	14.07	14.5
b	5.37	5.6
c	7.37	7.4
α	90.0	90.0
β	90.0	90.0
γ	90.0	90.0
Δ*b*[c]	0	0
Δ*c*[c]	0	0
CC bonds[d]	1.540, 1.540	1.542, 1.542
	1.543, 1.543	1.546, 1.546
	1.540, 1.540	1.542, 1.542
	1.543, 1.543	1.546, 1.546
CCC angles[d]	111.8, 115.9	111.7, 116.4
	111.8, 117.1	111.7, 117.2
	111.8, 115.9	111.7, 116.4
	111.8, 117.1	111.7, 117.2
CC torsions[d]	−173.7, −173.6	−174.3, −174.3
	57.2, 57.2	57.5, 57.5
	−173.7, −173.6	−174.3, −174.3
	57.2, 57.2	57.5, 57.5
energies		
E_0[cov][e]	0.74	0.79
E_0[vdW][f]	1.77	1.66
E_0[elec][g]	−11.88	−11.86
E_0[lat][h]	−4.21	−3.95
E_0	−13.58	−13.36
ΔE_0[i]	0.21	0.43
ΔE_z[j]	0.12	0.15

[a] Bond and unit cell lengths in angstroms; bond and unit cell angles, and torsions, in degrees. [b] Energies in kcal/mol/m.u. [c] Fractional unit cell shifts of *bc* sheets from $C222_1$ structure. [d] Main chain: first bond (corresponding to central bond of the first torsion) starts at CH−CH_2, first angle starts at same CH_2−CH−CH_2, first torsion starts at CH−CH_2 bond. [e] Energy of distortion of bonds, angles, and torsions (including cross-terms) of a single chain from intrinsic values.[38] [f] Intrachain van der Waals energy. [g] Intrachain electrostatic energy. [h] Interchain van der Waals plus electrostatic energy. [i] Energy relative to $E_0(0)$ of form I, **2B**. [j] Energy relative to $E_z(0)$ of form I, **1A**.

Table 4. Structures[a] and Energies[b] of Form III Crystalline Syndiotactic Polypropylene

	structure	
parameter	unconstrained	room temp
a	4.87	5.22
b	10.74	11.17
c	5.11	5.06
α	90.0	90.0
β	90.0	90.0
γ	90.0	90.0
CC bonds[c]	1.549, 1.549	1.543, 1.543
	1.549, 1.549	1.543, 1.543
CCC angles[c]	111.0, 113.5	110.2, 113.0
	111.0, 113.5	110.2, 113.0
CC torsions[c]	162.5, 162.5	161.7, 161.7
	−162.5, −162.5	−161.7, −161.7
energies		
E_0[cov][d]	1.22	1.14
E_0[vdW][e]	2.38	2.52
E_0[elec][f]	−11.91	−11.91
E_0[lat][g]	−4.84	−4.43
E_0	−13.15	−12.68
ΔE_0[h]	0.64	1.11
ΔE_z[i]	0.55	0.67

[a] Bond and unit cell lengths in angstroms; bond and unit cell angles, and torsions, in degrees. [b] Energies in kcal/mol/m.u. [c] Main chain: first bond (corresponding to central bond of the first torsion) starts at CH−CH_2, first angle starts at same CH_2−CH−CH_2, first torsion starts at CH−CH_2 bond. [d] Energy of distortion of bonds, angles, and torsions (including cross-terms) of a single chain from intrinsic values.[38] [e] Intrachain van der Waals energy. [f] Intrachain electrostatic energy. [g] Interchain van der Waals plus electrostatic energy. [h] Energy relative to $E_0(0)$ of form I, **2B**. [i] Energy relative to $E_z(0)$ of form I, **1A**.

this unit cell is only 0.12 kcal/mol/m.u. higher than that of form I, **1A**. The latter value indicates that two form II unit cells would have an energy of 1.9 kcal/mol higher than one form I, **1A**, cell.

The RT structure maintains the $t_1t_1g_1g_1t_1t_1g_1g_1$ chain conformation, although with slightly altered torsion angles. A comparison of its relative E_z(RT) value of 0.15 kcal/mol/m.u. with those of forms I, **1A**, **2A**, and **3A**, now shows that it would be favored over structures **2A** and **3A**, with only a ∼0.5 kcal/mol penalty for two unit cells compared to one form I, **1A**, cell. Of course, the situation is quite different if a defect in a *bc* sheet converts (say) an L into an R chain: the resulting sequence of three R chains might well favor the formation of form II unit cells in adjacent sheets. On the other hand, the usual formation of form II from form III crystals[19] presents no problem, particularly since the energy of the latter is much higher than that of the former (see below).

(c) Form III. As we have noted, form III crystals are obtained by cold drawing sPP samples that are quenched from the melt.[22] Their formation may be related to the unusually high fraction (up to 0.80) of trans segments in the sample just after quenching.[44] The latter, however, seems to be a mesophase, since the crystalline form III,[22] obtained on stretching, reverts to this less ordered phase when the tension is released.[45] Interestingly, in some samples (removed quickly from the quench) an oriented form I can be converted to form III by additional stress, with a reversion to form I when the tension is released. All of these observations indicate that form III is of higher energy than form I and can only be stabilized by external constraints.

Our calculations of the structures and energetics of form III crystals are given in Table 4. The chains in both unconstrained, and RT unit cells retain the t*cm* symmetry of the single-chain calculation (see Table 1), although the torsion angles differ from those previously calculated.[35] The chain axis repeat in the unconstrained cell is larger than in the RT cell, as expected,[40] in distinction to a previous calculation.[35] Nor do we find the "tilted" CH_3 groups proposed by the crystal structure analysis.[22] The energies of both unit cells are significantly higher than those of form I structures, primarily because the increase in intrachain energy (for the unconstrained, $\Delta E_0(0)[\text{tot}] = 1.08$ and for the RT, $\Delta E_0(\text{RT})[\text{tot}] = 1.16$ kcal/mol/m.u.) is not compensated by the decrease in interchain energy (for the unconstrained $\Delta E_0(0)[\text{lat}] = -0.49$, and for RT $\Delta E_0(\text{RT})[\text{lat}] = -0.40$ kcal/mol/m.u.). This higher energy is consistent with the observation that well-formed form III crystals are found only under the influence of an external stress on the chain.[45]

(d) Form IV. As noted above, several unit cells have been considered for the crystal structure of form IV sPP, including three triclinic[28] and one monoclinic.[30] Our calculations indicate that, for the unconstrained structures, there is no detectable difference in energy between the proposed triclinic[28] and the essentially identical monoclinic[30] structures. In both cases the *t*2 symmetry of the isolated chain is retained in the crystal. The only way of distinguishing between these structures would be through their vibrational spectra: although the in-phase frequencies of the two-chain monoclinic cell

Table 5. Structures[a] and Energies[b] of Form IV Crystalline Syndiotactic Polypropylene

	structure	
parameter	unconstrained	room temp
a	14.04	14.17
b	5.50	5.72
c	11.41	11.60
α	90.0	90.0
β	110.4	108.8
γ	90.0	90.0
CC bonds[c]	1.542, 1.543, 1.544, 1.544	1.544, 1.545, 1.546, 1.546
	1.543, 1.542, 1.542, 1.543	1.545, 1.544, 1.544, 1.545
	1.541, 1.541, 1.543, 1.542	1.544, 1.544, 1.545, 1.544
CCC angles[c]	112.4, 115.8, 109.2, 116.5	112.5, 115.9, 109.2, 116.7
	109.2, 115.8, 112.4, 117.5	109.2, 115.9, 112.5, 118.1
	112.5, 115.6, 112.5, 117.5	112.7, 115.6, 112.7, 118.1
CC torsions[c]	−177.2, −172.5, 178.6, 178.6	−177.6, −172.1, 178.5, 178.5
	−172.5, −177.2, 56.4, 52.9	−172.1, −177.6, 57.2, 54.9
	−176.7, −176.7, 52.9, 56.4	−178.7, −178.7, 54.9, 57.2
energies		
E_0[cov][d]	0.69	0.76
E_0[vdW][e]	1.88	1.77
E_0[elec][f]	−11.83	−11.81
E_0[lat][g]	−4.39	−4.14
E_0	−13.64	−13.42
ΔE_0[h]	0.15	0.37
ΔE_z[i]	0.11	0.11

[a] Bond and unit cell lengths in angstroms; bond and unit cell angles, and torsions, in degrees. [b] Energies in kcal/mol/m.u. [c] Main chain: first bond (corresponding to central bond of the first torsion) starts at $CH-CH_2$, first angle starts at same $CH_2-CH-CH_2$, first torsion starts at $CH-CH_2$. [d] Energy of distortion of bonds, angles, and torsions (including cross-terms) of a single chain from intrinsic values.[38] [e] Intrachain van der Waals energy. [f] Intrachain electrostatic energy. [g] Interchain van der Waals plus electrostatic energy. [h] Energy relative to $E_0(0)$ of form I, **2B**. [i] Energy relative to $E_z(0)$ of form I, **1A**.

Table 6. Relative Zero-Point-Corrected Energies[a] of Forms I−IV Syndiotactic Polypropylene Crystal Structures

	relative energies	
structures	unconstrained	room temp
form I		
1A	0	0.12
1B	0.21	0.36
2A	0.03	0.17
2B	0.00	0.30[b]
3A	0.10	0.19
3B	0.12	0.25
form II	0.12	0.15
form III	0.55	0.67
form IV	0.11	0.11

[a] In kcal/mol/m.u. with respect to that of form I, **1A**. [b] Structure has two imaginary frequencies.

are identical to those of the single-chain triclinic cell, the out-of-phase modes of the monoclinic cell can be significantly different. For example, in the region below 250 cm^{-1} the frequencies in the former case are 34.1, 38.7, 69.8, 78.8, 80.0, 105.6, 114.6, 124.5, 143.4, 144.3, 152.7, 181.4, 201.7, 220.2, 223.4, and 233.1 cm^{-1} whereas in the latter case they are 16.0, 30.6, 41.6, 49.7, 60.9, 73.7, 83.5, 87.9, 108.8, 109.4, 132.0, 136.2, 141.2, 160.2, 184.7, 198.8, 212.1, 217.3, and 240.8 cm^{-1}. For the RT structures, the energy of the monoclinic is ∼0.01 kcal/mol/m.u. lower than that of the triclinic, and the chain retains its *t*2 symmetry. We therefore believe, as proposed,[30] that the preferred form IV crystal structure will be monoclinic, and its parameters are given in Table 5.

Comparison of the $\Delta E_z(0)$ and ΔE_z(RT) of form IV with those of forms I and II (Tables 2 and 3) shows that this structure is energetically competitive with some of the latter, a conclusion not evident from the ΔE_0 values alone. This lends support to the idea that $(t_6g_2t_2g_2)$ sequences can form kink bands between regular $(t_2g_2)_2$ regions.[12,30] In this context, it is also understandable why the $(t_2)_2$ form III structure, with its significantly higher ΔE_z (Table 4), is not relatively stable and is clearly found only in stretched samples,[20−22] in fact relaxing back to the helical $(t_2g_2)_2$ conformation when the tension is released, a change, as surmised[46] and as shown by our calculations, that is primarily enthalpic in origin.

The relative zero-point-corrected energies of the various crystal forms are collected in Table 6.

Conclusions

The results of our energetics analysis of sPP crystal structures leads to a number of conclusions. First, relative energies need to be compared after potential energies at minima are corrected for their respective zero-point energies. This is particularly significant for sPP, some of whose possible crystal structures are very close in energy, and emphasizes the importance of a vibrationally competent energy function such as our SDFF.[38] Second, it is additionally clear, as noted earlier,[14,15] that the pure *Ibca* crystal structure of form I as originally proposed[4] is unstable (with one imaginary frequency) and for orthorhombic cells will reorganize in the directions of minima 1, 2, and 3 of Figure 4 in that energetic order (see Table 6). Although it has been suggested that the lowest energy structure (**1A**, Figure 5) is unlikely because of steric reasons,[4] the energetics indicate otherwise.[15] We also note that, because of the *bc* contact plane in the epitaxially grown sPP crystals, the atomic force microscopy results[6] only require alternation of R and L chains in this plane. The close energies of the various form I structures strengthen the supposition that the observed structure may involve a statistical mixture of these possibilities.[10,14,15]

Third, with a form II energy at RT being second to the lowest form I structure, the formation of form II under certain conditions can be justified. Fourth, the comparable energies of the form IV crystal structure (which we support as monoclinic[30]) and some of the form I structures make it understandable, as suggested,[12,30] that $(t_6g_2t_2g_2)$ sequences could constitute kink bands between $(t_2g_2)_2$ regions. Finally, the significantly higher energy of the form III unit cell can account for the appearance of this structure only under conditions of external stress.

Acknowledgment. This research was supported by NSF Grant DMR 9902727.

References and Notes

(1) Natta, G.; Pasquon, I.; Corradini, P.; Peraldo, M.; Pegoraro, M.; Zambelli, A. *Rend. Accad. Naz. Lincei* **1960**, *28*, 539−544.
(2) Natta, G.; Corradini, P.; Ganis, P. *Makromol. Chem.* **1960**, *39*, 238−242.
(3) Corradini, P.; Natta, G.; Ganis, P.; Temussi, P. A. *J. Polym. Sci., Part C* **1967**, *16*, 2477−2484.
(4) Lotz, B.; Lovinger, A. J.; Cais, R. E. *Macromolecules* **1988**, *21*, 2375−2382.
(5) Lovinger, A. J.; Lotz, B.; Davies, D. D.; Padden, F. J., Jr. *Macromolecules* **1993**, *26*, 3494−3503.
(6) Stocker, W.; Schumacher, M.; Graff, S.; Lang, J.; Wittman, J. C.; Lovinger, A. J.; Lotz, B. *Macromolecules* **1994**, *27*, 6948−6955.
(7) De Rosa, C.; Corradini, P. *Macromolecules* **1993**, *26*, 5711−5718.
(8) Auriemma, F.; De Rosa, C.; Corradini, P. *Macromolecules* **1993**, *26*, 5719−5725.
(9) De Rosa, C.; Auriemma, F.; Corradini, P. *Macromolecules* **1996**, *29*, 7452−7459.
(10) De Rosa, C.; Auriemma, F.; Vinti, V. *Macromolecules* **1997**, *30*, 4137−4146.
(11) Sozzani, P.; Simonutti, R.; Galimberti, M. *Macromolecules* **1993** *26*, 5782−5789.
(12) Auriemma, F.; Born, R.; Spiess, H. W.; De Rosa, C.; Corradini, P. *Macromolecules* **1995**, *28*, 6902−6910.
(13) Auriemma, F.; Lewis, R. H. Spiess, H. W. *Macromol. Chem. Phys.* **1995**, *196*, 4011−4024.
(14) Lacks, D. J. *Macromolecules* **1996**, *29*, 1849−1851.
(15) Palmo, K.; Krimm, S. *Macromolecules* **1996**, *29*, 8549−8550.
(16) Lovinger, A. J.; Lotz, B. *J. Polym. Sci., Part B: Polym. Phys.* **1997**, *35*, 2523−2533.
(17) Auriemma, F.; De Rosa, C.; Ruiz de Ballesteros, O.; Corradini, P. *Macromolecules* **1997**, *30*, 6586−6591.
(18) De Rosa, C.; Auriemma, F.; Vinti, V. *Macromolecules* **1998**, *31*, 7430−7435.
(19) Lotz, B.; Mathieu, C.; Thierry, A.; Lovinger, A. J.; De Rosa, C.; Ruiz de Ballesteros, O.; Auriemma, F. *Macromolecules* **1998**, *31*, 9253−9257.
(20) Natta, G.; Peraldo, M.; Allegra, G. *Makromol. Chem.* **1964**, *75*, 215−216.
(21) Tadokoro, H.; Kobayashi, M.; Kobayashi, S.; Yasufuku, K.; Mori, K. *Rep. Prog. Polym. Phys. Jpn.* **1966**, *9*, 181−184.
(22) Chatani, Y.; Maruyama, H.; Noguchi, K.; Asanuma, T.; Shiomura, T. *J. Polym. Sci., Part C: Polym. Lett.* **1990**, *28*, 393−398.
(23) Nakaoki, T.; Ohira, Y.; Hayashi, H.; Horii, F. *Macromolecules* **1998**, *31*, 2705−2706.
(24) Ohira, Y.; Horii, F.; Nakaoki, T. *Macromolecules* **2000**, *33*, 1801−1806.
(25) Nakaoki, T.; Yamanaka, T.; Ohira, Y.; Horii, F. *Macromolecules* **2000**, *33*, 2718−2721.
(26) Ohira, Y.; Horii, F.; Nakaoki, T. *Macromolecules* **2000**, *33*, 5566−5573.
(27) Vittoria, V.; Guadagno, L.; Comotti, A.; Simonutti, R.; Auriemma, F.; De Rosa, C. *Macromolecules* **2000**, *33*, 6200−6204.
(28) Chatani, Y.; Maruyama, H.; Asanuma, T.; Shiomura, T. *J. Polym. Sci., Part B: Polym. Phys.* **1991**, *29*, 1649−1652.
(29) Asakura, T.; Aoki, A.; Date, T.; Demura, M.; Asanuma, T. *Polym. J.* **1996**, *28*, 24−29.
(30) Auriemma, F.; De Rosa, C.; Ruiz de Ballesteros, O.; Vinti, V.; Corradini, P. *J. Polym. Sci., Part B: Polym. Phys.* **1998**, *36*, 395−402.
(31) Natta, G.; Corradini, P.; Ganis, P. *J. Polym. Sci.* **1962**, *58*, 1191−1199.
(32) Corradini, P.; Napolitano, R.; Petraccone, V.; Pirozzi, B.; Tuzi, A. *Macromolecules* **1982**, *15*, 1207−1210.
(33) Suter, U. W.; Flory, P. J. *Macromolecules* **1975**, *8*, 765−776.
(34) Corradini, P.; Napolitano, R.; Pirozzi, B. *Rend. Fis. Acc. Lincei* **1991**, *2*, 341−352.
(35) Pirozzi, B.; Napolitano, R. *Eur. Polym. J.* **1992**, *28*, 703−708.
(36) Napolitano, R.; Pirozzi, B. *Polymer* **1997**, *38*, 4847−4853.
(37) Palmo, K.; Pietila, L.-O.; Krimm, S. *J. Comput. Chem.* **1991**, *12*, 385−390.
(38) Palmo, K.; Mirkin, N. G.; Krimm, S. *J. Phys. Chem. A* **1998**, *102*, 6448−6456.
(39) Palmo, K.; Krimm, S., to be published.
(40) Lacks, D. J.; Rutledge, G. C. *J. Phys. Chem.* **1994**, *98*, 1222−1231.
(41) Peraldo, M.; Cambini, M. *Spectrochim. Acta* **1965**, *21*, 1509−1525.
(42) Masetti, G.; Cabassi, F.; Zerbi, G. *Polymer* **1980**, *21*, 143−152.
(43) Schachtschneider, J. H.; Snyder, R. G. *Spectrochim. Acta* **1965**, *21*, 1527−1542.
(44) Ohira, Y.; Horii, F.; Nakaoki, T. *Macromolecules* **2001**, *34*, 1655−1662.
(45) Guadagno, L.; D'Aniello, C.; Naddeo, C.; Vittoria, V. *Macromolecules* **2001**, *34*, 2512−2521.
(46) Auriemma, F.; Ruiz de Ballesteros, O.; De Rosa, C. *Macromolecules* **2001**, *34*, 4485−4491.

MA011230G